New Phytologist

The unicellular green microalga *Botryosphaerella sudetica* links plant-like light protection with an algal lifestyle

Olga Blifernez-Klassen[1], Hanna Berger[2], Viktor Klassen[1], Swapnil Chaudhari[3], Thomas Baier[1], Lutz Wobbe[1] and Olaf Kruse[1]

[1]Algae Biotechnology and Bioenergy, Faculty of Biology, Center for Biotechnology (CeBiTec), Bielefeld University, Universitätsstrasse 27, 33615, Bielefeld, Germany; [2]Die Blattmacher Kommunikation und Wissenschaft GmbH, Försterweg 2, 14482, Potsdam, Germany; [3]Sartorius Stedim Biotech GmbH, August Spindler Str. 11, 37079, Goettingen, Germany

Authors for correspondence:
Olaf Kruse
Email: olaf.kruse@uni-bielefeld.de

Olga Blifernez-Klassen
Email: olga.blifernez@uni-bielefeld.de

Received: *18 July 2025*
Accepted: *2 January 2026*

New Phytologist (2026) **251:** 372–383
doi: 10.1111/nph.70990

Key words: *Botryosphaerella sudetica*, *Chlamydomonas reinhardtii*, microalgae, nonphotochemical quenching, photoprotection.

Summary

- Nonphotochemical quenching (NPQ) mechanisms fine-tune light utilisation in the photosynthetic antenna, for example, in response to excess light, to prevent photodamage. NPQ comprises distinct mechanisms, all contributing to photoprotection but acting on different time scales. Preferences for individual mechanisms and NPQ composition are proposed to reflect the organism's lifestyle, especially regarding sessile vs motile styles, with the latter enabling photophobic responses. We analysed photoprotection in the nonmotile, unicellular chlorophycean microalga *Botryosphaerella sudetica*, belonging to a genus known to form high-light-exposed floating aquatic biofilms.
- Growth, Chl fluorescence, its nuclear genome, and the expression of photoprotective genes were analysed in comparison with the motile chlorophycean microalga *Chlamydomonas reinhardtii*.
- These analyses revealed that *B. sudetica* is, in contrast to *C. reinhardtii*, equipped with a constitutive energy-dependent quenching (qE) mechanism based on the constitutive accumulation of protein PSBS, the thylakoid lumen pH-sensor, found throughout the green plant lineage. While qE was the predominant NPQ mechanism in *B. sudetica* and required zeaxanthin formation, state transitions (qT), which largely contributed to NPQ in *C. reinhardtii*, played a minor role.
- These data demonstrate that a core set of NPQ mechanisms conserved in the *Viridiplantae* is shuffled to meet better the adaptive requirements imposed by the habitat.

Introduction

Vascular plants and simple unicellular microalgae are equipped with photoprotective mechanisms, which help avoid an over-excitation of Photosystem II (PSII) and resulting photoinhibition under conditions when photosynthesis becomes oversaturated. Among the photoprotective mechanisms is the so-called nonphotochemical quenching (NPQ), a collective term covering several distinct mechanisms all contributing to a reduction of Chla fluorescence as a result of short-term acclimation (Wobbe *et al.*, 2016). At least five different NPQ mechanisms can be distinguished according to the time scale they operate on.

The most rapid mechanism, operating in the range of seconds to minutes, is ascribed to energy dissipation (qE), and is regulated by the pH gradient across the thylakoid membrane (ΔpH). On a time scale of minutes, the de-epoxidation of violaxanthin generates zeaxanthin, a pigment whose binding to LHC antenna proteins (Niyogi *et al.*, 1997a, 1997b) induces zeaxanthin-dependent quenching (qZ). State transitions (qT), acting also on the minute time scale, rapidly reduce the absorbance cross-section at PSII by decoupling part of the associated light-harvesting antenna, thus contributing to PSII protection and fluorescence quenching. This process requires the reversible phosphorylation of light-harvesting proteins associated with PSII (LHCII; Rochaix, 2011; Goldschmidt-Clermont & Bassi, 2015). In addition to those mentioned above, there are two slowly reversible NPQ components, qH, localised to the LHCII antenna (Malnoë *et al.*, 2018) and qI, which can be caused by D1 photodamage (Edelman & Mattoo, 2008).

Based on studies conducted with the two eukaryotic model organisms for photosynthesis research within the green plant lineage, *Arabidopsis thaliana* and *Chlamydomonas reinhardtii*, two distinct types of energy-dependent quenching (qE) were identified. The rapidly activatable energy-dependent quenching, known for sessile land plants, relies on the constitutive expression of the pigment-less pH-sensor Photosystem II subunit S (PSBS) (Li *et al.*, 2004), and has already been characterised in vascular plants (Li *et al.*, 2000) and the moss *Physcomitrella patens* (Alboresi *et al.*, 2010). A different qE mechanism was demonstrated for the green microalga *C. reinhardtii*, which is based on the inducible expression of light-harvesting complex stress-related (*LHCSR*) genes, encoding Chl/carotenoid-binding

© 2026 The Author(s).
New Phytologist © 2026 New Phytologist Foundation.
This is an open access article under the terms of the Creative Commons Attribution License, which permits use, distribution and reproduction in any medium, provided the original work is properly cited.

proteins with three transmembrane helices (Bonente *et al.*, 2011; Liguori *et al.*, 2013). Expression of these genes is induced by high light (Peers *et al.*, 2009), and even at low intensities by UV-B (Allorent *et al.*, 2016; Redekop *et al.*, 2022) and blue light (Petroutsos *et al.*, 2016; Redekop *et al.*, 2022). In addition to light, cellular carbon dioxide levels regulate the accumulation of LHCSR proteins, with LHCSR3 accumulation being strongly repressed by high intracellular carbon dioxide concentrations (Ruiz-Sola *et al.*, 2023). Inactivation of the genes *LHCSR3.1* and *LHCSR3.2* encoding identical proteins leads to a loss of most qE (Peers *et al.*, 2009), at least in the absence of UV-B light (Allorent *et al.*, 2016), whereas the qE reduction observed following *LHCSR1* knock-out is rather mild (Truong, 2011). Recently, it was proposed that the major light-harvesting protein LHCBM1, whose knock-out diminishes qE (Elrad *et al.*, 2002), links LHCSR3 to the PSII supercomplex (Liu *et al.*, 2024). In the moss *Physcomitrella patens*, functional LHCRS protein accumulates along with PSBS (Alboresi *et al.*, 2010).

The nuclear genome of *C. reinhardtii* also contains two PSBS genes, encoding proteins that only differ by one amino acid (Bonente *et al.*, 2008). Their accumulation following high-light exposure is only transient and cannot compensate for a loss of LHCSR3 (Correa-Galvis *et al.*, 2016; Tibiletti *et al.*, 2016). In *C. reinhardtii*, PSBS accumulation is controlled by CO_2 availability, with low CO_2 conditions enabling PSBS detection for several hours after exposure to HL and rapid degradation after *c.* 1 h at high CO_2 levels (Correa-Galvis *et al.*, 2016). Although PSBS alone is not sufficient for functional qE in *Chlamydomonas* (Correa-Galvis *et al.*, 2016), its overexpression, together with LHCSR proteins, increases NPQ capacity and cell viability under HL conditions (Wilson *et al.*, 2023). Lower PsbS amounts negatively affect high-light acclimation by harming NPQ capacity, electron transport characteristics, antenna organisation and morphological changes, resulting in an increased HL sensitivity. Although higher PsbS amounts do not result in a higher NPQ capacity, they nevertheless provide higher fitness and tolerance towards HL stress. It was proposed that PsbS is transiently required during HL acclimation to facilitate thylakoid membrane and antenna protein reorganisation along with NPQ activation and adjustments in the electron transport chain, and that degradation of PsbS is essential for functional HL acclimation (Redekop *et al.*, 2020).

In contrast to sessile land plants, many microalgal species are equipped with flagella for photophobic responses (Kröger & Hegemann, 1994), representing an efficient means to reduce light stress exposure and a potential explanation for the lack of constitutive qE mechanisms in flagellated microalgae, such as *C. reinhardtii*. An analysis of six different green algal species by Quaas *et al.* indicated that NPQ mechanisms differ in terms of their xanthophyll cycle dependence and preacclimation requirement for full NPQ induction (Quaas *et al.*, 2015). To get insights into potential differences between members of the clade of *Chlorophyceae* (including *C. reinhardtii*) in terms of photoprotective strategies applied, we analysed short-term acclimation mechanisms in the green microalga *Botryosphaerella sudetica* (synonym *Botryococcus sudeticus* (Vazquez-Duhalt & Greppin, 1987); Class: Chlorophyceae; Order: Sphaeropleales; Family: Neochloridaceae; Genus Botryosphaerella (Silva, 1980)) towards excess light.

Materials and Methods

Strains and culture conditions

Botryosphaerella sudetica Lemm. (Silva, 1970) was isolated from the consortium surrounding the green microalga *Botryococcus braunii* var. Showa culture, obtained from the Berkeley culture collection. *Chlamydomonas reinhardtii* cc1690 was used as a reference strain. Algae were grown at 25°C under photoautotrophic conditions in Chu medium (without vitamins and citric acid) gassed with moisture presaturated carbon dioxide-enriched air (5%, v/v) (Blifernez-Klassen *et al.*, 2021), except when stated otherwise. Three synchronised microalgal cultures per strain were used as inoculum for three biological replicates. Synchronisation of the cultures was achieved by growing the cells under 12 : 12, light : dark illumination of 100 µmol photons m^{-2} s^{-1} white light for 3 wk, with subsequent dilution to a culture density of *c.* 10^6 cells ml^{-1} every 3–4 d. For the main experiments, continuous white light intensities of 100 (low light), 400 (moderate–high light), and 1000 (high light) µmol photons m^{-2} s^{-1} were used. Culture growth was monitored by measurements of biomass organic dry weight (oDW) as described previously (Klassen *et al.*, 2017).

Chlorophyll fluorescence analyses and oxygen evolution capacity measurements

For all fluorescence analyses as well as oxygen evolution measurements, algae cultures at a Chl concentration of *c.* 10 µg ml^{-1} were used. Chlorophyll concentration was measured as described before (Blifernez-Klassen *et al.*, 2018). *In vivo* oxygen evolution activity measurements were performed according to Mussgnug *et al.* (2007) with cells acclimated to either 100 (LL) or 1000 (HL) µmol m^{-2} s^{-1} for 2 d and using 1400 µmol photons m^{-2} s^{-1} actinic white light in the presence of 10 mM $NaHCO_3$ and using a Clark-type oxygen electrode. For Chl fluorescence measurements, the cultures were dark-adapted for at least 1 h, and measurements were performed using MiniPam (Waltz) or VideoImager (PSI, Photon Systems Instruments, Brno, Czech Republic) as described (Maxwell & Johnson, 2000; Murchie & Lawson, 2013). White actinic light used was 10, 100, 400, and 1000 µmol m^{-2} s^{-1} (MiniPAM) and 1100 µmol m^{-2} s^{-1} (VideoImager). State 1 and State 2 were obtained by incubating algae cultures with 20 µM DCMU or 250 µM NaN_3 for 20 min. The NPQ parameters qI, qT, and qE were measured and calculated as in Quaas *et al.* (2015). Dithiothreitol (DTT; 1 mM) was used as an inhibitor of the enzyme violaxanthin-de-epoxidase. For fluorescence emission at 77 K, samples directly from cultures or in State 1 or 2, respectively, were frozen in liquid nitrogen and spectra were recorded using an excitation wavelength of 480 nm (Kruse *et al.*, 1999).

© 2026 The Author(s).
New Phytologist © 2026 New Phytologist Foundation.

RNA isolation and quantitative real-time RT-PCR

Total RNA was isolated using the Quick-RNA Plant Miniprep Kit (Zymo Research, Irvine, CA, USA) according to the manufacturer's instructions. Reverse transcription quantitative quantitative polymerase chain (RT-qPCR) was carried out using the SensiFastTM SYBR Hi-ROX One-Step Kit (Bioline Reagents Ltd, London, UK), as described before (Wobbe *et al.*, 2009) using the primer presented in Supporting Information Table S1.

Gel electrophoresis and immunoblot

Immunoblotting was performed as described (Berger *et al.*, 2016), and the total cellular protein amount was determined by the Lowry assay (Bio-Rad). Immunodetection was performed using enhanced chemiluminescence (GE Health Care, Chicago, IL, USA). The rabbit polyclonal anti-LHCSR3 antiserum was raised against a KLH-conjugated synthetic peptide derived from the LHCSR3 protein sequence (UniProt P0DO18) from *Chlamydomonas reinhardtii* and was purchased from Agrisera (AS14 2766). The rabbit polyclonal anti-PSBS antiserum was raised against barley (*Hordeum vulgare*) PsbS protein and was a kind gift from R. Bassi (Bonente *et al.*, 2008). For densitometric quantification, the software ImageJ was used.

Pigment analysis via UV–vis-HPLC

Pigment analyses were performed according to the protocols described before (Blifernez-Klassen *et al.*, 2018).

Immunoblot analysis of recombinant Bs-PSBS and Bs-LHCSR proteins

The coding sequences of *B. sudetica* PSBS and LHCSR were codon-optimised for *E. coli* and synthesised (Genscript) with a His-tag of eight amino acids. Cloning was performed using the restriction enzymes NdeI and XhoI before ligation into the vector pET24a(+) (Novagen, Madison, WI, USA). Transformation of chemically competent *E. coli* KRX (Promega) cells (LHCSR) or BL21 (PSBS) was performed via the heat shock method, with subsequent selection on Luria Bertani plates containing 50 mg l^{-1} kanamycin. Protein production was induced by either the addition of 0.1% (w/v) rhamnose at OD600 *c.* 0.4 (KRX/LHCSR) or 0.5 mM Isopropyl β-d-1-thiogalactopyranoside (BL21/PSBS) and subsequent cultivation overnight at 24°C. Untransformed *E. coli* cells or cells containing an empty vector were used as controls. Cells were harvested via centrifugation (5000 ***g***, 10 min, 4°C), resuspended in cold phosphate-buffered saline (pH 7.4) with cOmplete™ Protease Inhibitor Cocktail (Merck) and lysed via sonication. After centrifugation (18 000 ***g***, 10 min, 4°C), soluble protein fraction (supernatant, SF) and insoluble protein extracts (Pellet, UE) were supplemented with SDS-sample buffer and separated by sodium dodecyl sulphate–polyacrylamide gel electrophoresis (SDS-PAGE) and applied for immunoblot analyses with αHis$_6$, αLHCSR3, or αPSBS antisera. 2,2,2-trichloroethanol in-gel visualisation or Coomassie Brilliant Blue staining was used as a loading control (Blifernez-Klassen *et al.*, 2021).

Statistical analysis

Results were shown either as mean value or fold change of mean values; error bars represent SD or SE of mean (SD/SEM, $n = 3$). Statistical analysis was performed with two-tailed Student's *t*-test, resulting in p-values indicated by asterisks (*, $P \leq 0.05$; **, $P \leq 0.01$).

Results

A comparative growth analysis of *B. sudetica* (Fig. 1a) and *C. reinhardtii* (Fig. 1b) revealed substantial differences in the light tolerance of both species. When low cell density inoculates of *B. sudetica* and *C. reinhardtii* were cultivated at high-light intensity (Fig. 1a,b; HL), *B. sudetica* displayed a much higher maximal productivity (P_{max} = 0.618 ± 0.037 g l^{-1} d^{-1}) than *C. reinhardtii* (P_{max} = 0.143 ± 0.017 g L^{-1} d^{-1}), resulting in an up to 2.5 times higher biomass accumulation noted for *B. sudetica* (Fig. 1a; left *y*-axis; white squares) compared with *C. reinhardtii* (Fig. 1b; white circles) in the stationary phase. An increased growth rate of *B. sudetica* under high-light conditions was also reflected by a significantly ($P < 0.05$) higher maximum PSII quantum yield (Fig. 1c; left *y*-axis; F_v/F_m; HL; 0.69 in *B.s.* vs 0.54 in *C.r.*) and *c.* 30% higher oxygen evolution rate than *C. reinhardtii* (Fig. 1d, HL), indicating that *B. sudetica* is less susceptible to photoinhibition. Under the growth conditions applied, cells of *B. sudetica* were not flagellated, as light microscopic images revealed (Fig. S1).

To analyse whether the elevated light tolerance of *B. sudetica* is a result of its photoprotective mechanisms being more efficient than those active in *C. reinhardtii*, we determined the maximal NPQ (Fig. 2a) in low-light- and high-light-acclimated samples of both strains at different actinic light intensities. Following previous studies (Bonente *et al.*, 2011; Allorent *et al.*, 2013; Quaas *et al.*, 2015), an acclimation of *C. reinhardtii* to high light increased NPQ_{max} by up to 69% (*C.r.*; LL vs HL; 400 and 1000 µmol m^{-2} s^{-1}; $P < 0.05$), while the difference between NPQ_{max} was statistically insignificant ($P > 0.05$) when low-light- and high-light-acclimated *B. sudetica* cells were analysed (*B.s.*; LL vs HL; 400 and 1000 µmol m^{-2} s^{-1}).

These data indicated that, in contrast to *C. reinhardtii*, *B. sudetica* is equipped with a constitutive high NPQ capacity. To get further insights into the differences between both organisms regarding their preferred NPQ mechanisms, we analysed the kinetics of NPQ induction in more detail (Fig. 2b). In contrast to low-light (100 µmol photons m^{-2} s^{-1})-acclimated *C. reinhardtii* cultures, where the overall NPQ developed during actinic light illumination remained on a low level (*c.* 0.25; Cr LL), *B. sudetica* displayed a rapid plant-like increase in NPQ within 5 min, which exceeded the NPQ determined for *C. reinhardtii* about sevenfold (B.s. LL; 1.8 vs 0.25 in C.r.). Acclimation of *C. reinhardtii* to high light of 1000 µmol photons m^{-2} s^{-1} diminished the relative NPQ difference between both organisms, based on the light induction of NPQ, which has already been

© 2026 The Author(s).
New Phytologist © 2026 New Phytologist Foundation.

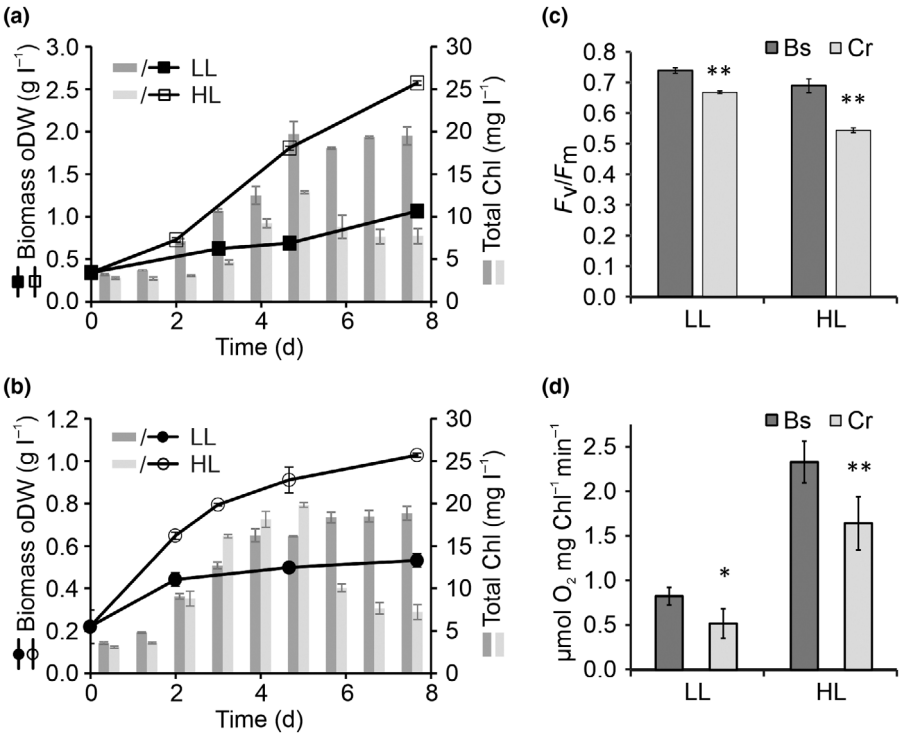


Fig. 1 *Botryosphaerella sudetica* is more light-tolerant than *Chlamydomonas reinhardtii*. (a) Growth curve of *B. sudetica* grown photoautotrophically at 100 µmol photons m^{-2} s^{-1} (low light; LL) or 1000 µmol photons m^{-2} s^{-1} (high light; HL) with 5% (v/v) carbon dioxide. Biomass accumulation determined as organic dry weight (DW; circles) is indicated on the left *y*-axis, and the Chl concentration (bars) in LL- and HL-grown cultures is shown on the right *y*-axis. Results are means ± SE (n = 3). (b) As in (a), but the growth experiment was conducted with *C. reinhardtii*. (c) Maximum quantum efficiency of Photosystem II recorded in the dark (F_v/F_m; grey bars) determined for cells acclimated to either LL or HL for 2 d. Results are means ± SE (n = 3). (d) Photosynthetic oxygen evolution rate of low-light (LL)- and high-light (HL)-acclimated cells of *B. sudetica* (Bs) and *C. reinhardtii* (Cr). Results are means ± SD (n = 3). Asterisks indicate results from a two-tailed Student's *t*-test for the comparison Cr with Bs (*, $P \leq 0.05$; **, $P \leq 0.01$).

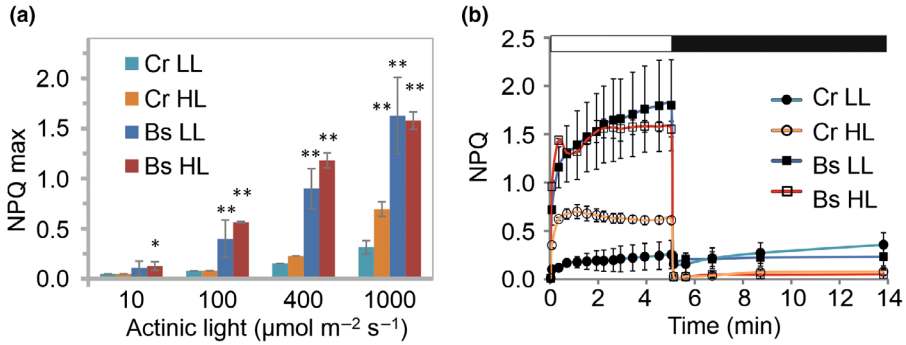


Fig. 2 *Botryosphaerella sudetica* is equipped with a plant-like, immediately available energy-dependent quenching capacity. (a) Nonphotochemical quenching capacity of *Chlamydomonas reinhardtii* (Cr) and *B. sudetica* (Bs) grown phototrophically (5% (v/v) CO_2) either under low-light (LL; 100 µmol photons m^{-2} s^{-1}) or high-light (HL; 1000 µmol photons m^{-2} s^{-1}) conditions. Nonphotochemical quenching (NPQ) was determined at distinct actinic light intensities indicated on the *x*-axis. Values represent mean values ± SD (n = 3). Asterisks indicate results from a two-tailed Student's *t*-test for the comparison with Cr LL (*, $P \leq 0.05$; **, $P \leq 0.01$) (b) NPQ induction *B. sudetica* and *C. reinhardtii* after growth under LL (100 µmol photons m^{-2} s^{-1}) or HL (1000 µmol photons m^{-2} s^{-1}). NPQ was determined during 5 min of illumination at 1100 µmol photons m^{-2} s^{-1} and a subsequent dark period of 9 min. Values represent means ± SD (n = 3).

described in previous studies (Bonente *et al.*, 2011; Allorent *et al.*, 2013; Quaas *et al.*, 2015).

Since at least three distinct types of quenching contribute to the overall NPQ capacity (Müller *et al.*, 2001), NPQ relaxation kinetics were recorded to disentangle the individual contributions of qT (state transitions), qI (photoinhibition), and energy-dependent quenching (qE; Figs 3a, S2). *B. sudetica* cultures were transferred from low light (100 µmol photons m^{-2} s^{-1}) to moderate–high light (MHL; 400 µmol photons m^{-2} s^{-1}) and cultivated photoautotrophically at this elevated light intensity. The fraction of qE increased during the cultivation experiment from *c.* 42% to *c.* 73%, representing the dominating NPQ type at the end of the cultivation period (Fig. 3a; green curve; qE). At the same time, the relative contribution of qI (red curve) decreased (from 47% to 21%), while state transitions (blue curve, Fig. 3a) contributed only marginally (*c.* 10%) to NPQ during the entire time course.

For *C. reinhardtii*, however, it was difficult to disentangle the distinct contributions of the NPQ components based on dark relaxation kinetics, which was due to a very slow recovery of Fm' in the dark, observed only for this organism (Fig. S2) and pointing to qT as the more relevant NPQ component.

© 2026 The Author(s).
New Phytologist © 2026 New Phytologist Foundation.

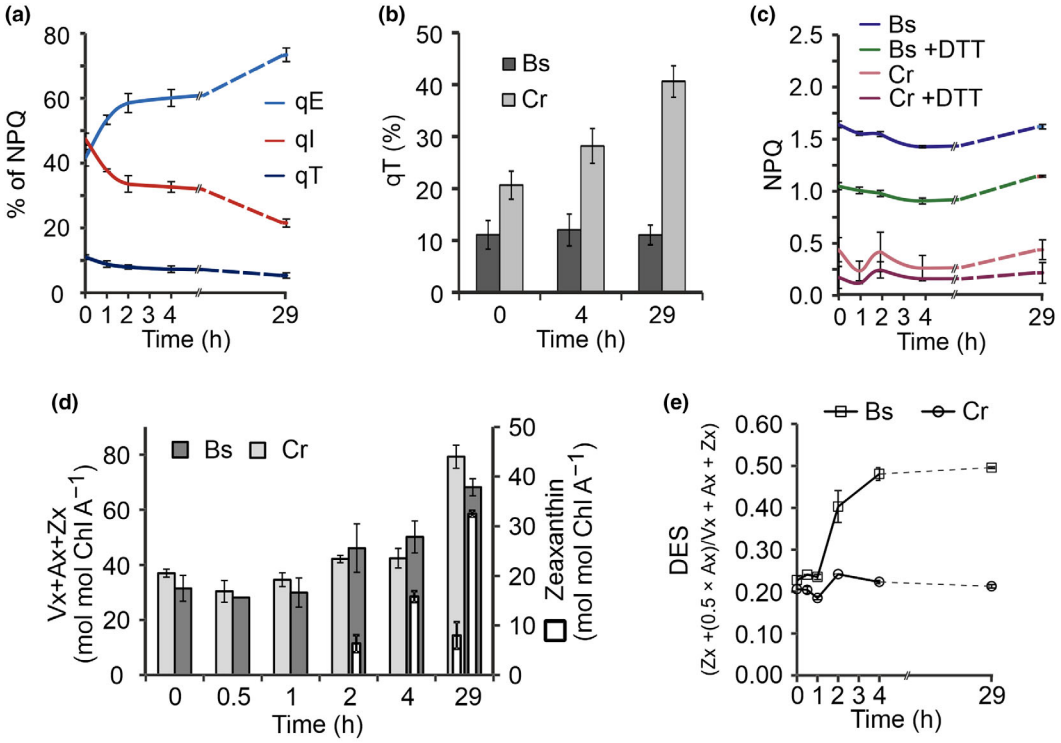


Fig. 3 Energy-dependent quenching (qE) is the dominant component of nonphotochemical quenching (NPQ) in *Botryosphaerella sudetica*. (a) Analysis of the individual contributions (% of NPQ) of qE (green curve), qT (black curve), and qI (red curve) to the total NPQ in *B. sudetica*. After induction of NPQ, dark relaxation kinetics were recorded to discriminate between NPQ components. Samples were taken from LL (100 μmol photons m^{-2} s^{-1}; t_0)- or moderate HL (400 μmol photons m^{-2} s^{-1})-acclimated cultures. (b) The fraction of qT (state transitions) contributing to NPQ in *Chlamydomonas reinhardtii* and *B. sudetica*, as determined from the PSII-LHC:PSI-LHC peak height ratio. (c) Violaxanthin de-epoxidase (VDE)-dependence of NPQ in *C. reinhardtii* and *B. sudetica* analysed by adding dithiothreitol (+DTT, 1 mM) as an inhibitor of the enzyme. (d) Violaxanthin cycle pool size (left *y*-axis) in *C. reinhardtii* (Cr) and *B. sudetica* (Bs), encompassing the relative cellular contents (mmol xanthophyll per mol of Chla) for violaxanthin (Vx), antheraxanthin (Ax), and zeaxanthin (Zx). The relative zeaxanthin content is indicated on the right *y*-axis. (e) De-epoxidation state (DES) of the violaxanthin cycle. Results are means ± SD from two biological replicates each, including two technical replicates (n = 2). PSII, Photosystem II.

To obtain additional insights into differences between *C. reinhardtii* and *B. sudetica* regarding the state transition process, we applied 77 K fluorescence spectroscopy to LL (t_0)- and moderate–high light (t_{4h}, t_{29h})-acclimated cells of both organisms (Fig. S3). *C. reinhardtii* displayed the typical Chl fluorescence curve with emission maxima recorded at 685 nm (PSII-LHCII complexes) and 712 nm (PSI-LHCI complexes). For all three time points, a transition from State 1 to State 2 was accompanied by a substantial decrease in the PSII-LHCII fluorescence and a moderate increase in the PSI-LHCI fluorescence in *C. reinhardtii*. The massive decline in the PSII-LHCII fluorescence during the State 1-to-State 2 transition has been described before and can be regarded as an effective means to rapidly protect PSII under conditions associated with high excitation pressure (Allorent *et al.*, 2013; Berger *et al.*, 2014; Ünlü *et al.*, 2014). The fluorescence spectra recorded for *B. sudetica* differed from those obtained for *C. reinhardtii* by containing an additional peak at *c.* 704 nm besides the PSII-LHCII (685 nm) and the PSI-LHCI (712 nm) peaks. This additional peak might either represent LHCI (Wollman & Bennoun, 1982) or LHCII (Wollman & Delepelaire, 1984) proteins not associated with their respective photosystems. Except for time point t_{29h}, *B. sudetica* State 1-to-State 2 transitions were characterised by an almost unchanged fluorescence of PSII-LHCII, indicating that, in contrast to *C. reinhardtii*, decoupling of LHCII from PSII occurs to a much lesser extent in *B. sudetica* and explains the low contribution of qT to NPQ (Fig. 3b, *Bs*). Inspection of the fluorescence spectra recorded with *C. reinhardtii* cells directly taken from the culture and not acclimated to a specific state (upper panels, t_0, t_4, t_{29}) revealed that changes in the relative fluorescence of PSII-LHCII and PSI-LHCI occurred during long-term high-light acclimation, with a higher PSI-LHCI:PSII-LHCII fluorescence ratio only observed following long-term exposure to excess light. A contrasting behaviour was seen for *B. sudetica*, both in terms of State 1-to-State 2 transitions and long-term acclimation to light stress (lower panels). While the reduction in PSII-LHCII fluorescence was only moderate in *B. sudetica*, a strong decline in the PSI-LHCI fluorescence was noted upon the transition to State 2. Regarding long-term effects, extended exposure to high light resulted in a balanced PSII-LHCII and PSI-LHCI fluorescence starting at a ratio shifted towards PSI-LHCI at t_0. If the reduction of PSI-LHCI fluorescence during the transition to State 2 reflects the dissociation of antenna proteins from PSI as a strategy to protect PSI, it cannot be answered at the moment. Overall, the

© 2026 The Author(s).
New Phytologist © 2026 New Phytologist Foundation.

Table 1 Light-harvesting and photoprotective proteins found in *Botryosphaerella sudetica* in comparison with the two model organisms for eukaryotic photosynthesis, *Arabidopsis thaliana*, and *Chlamydomonas reinhardtii*.

Description	Gene name	Gene ID Bs	Identity	Query cover	*E*-value	Compared to	UniProt KB
LHC proteins putatively associated with PSI							
	LHCA1	g5794.t1	50%	89%	1e-61	*At*_LHCA1	Q01667
			78%	100%	1e-127	*Cr*_LHCA1	Q05093
	LHCA2	g5900.t1	49%	76%	1e-66	*At*_LHCA4	P27521
			73%	99%	2e-128	*Cr*_LHCA2	A8IKC8
		g14955.t1	58%	67%	1e-27	*At*_LHCA4	P27521
			56%	80%	4e-22	*At*_LHCA2	Q9SYW8
			75%	94%	1e-55	*Cr*_LHCA4	Q75VZ0
	LHCA3	g6308.t1	64%	79%	2e-97	*At*_LHCA3	Q9SY97
			73%	97%	1e-144	*Cr*_LHCA3	Q75VY9
		g4199.t1	48%	47%	3e-64	*At*_LHCA3	Q9SY97
			43%	53%	2e-59	*Cr*_LHCA3	Q75VY9
	LHCA4	g7915.t1	49%	76%	4e-64	*At*_LHCA4	P27521
			73%	89%	3e-138	*Cr*_LHCA5	Q75VY8
		g14940.t1	48%	73%	7e-63	*At*_LHCA4	P27521
			69%	93%	3e-130	*Cr*_LHCA6	Q75VY6
	LHCA5	g14308.1	49%	87%	1e-65	*At*_LHCA2	Q9SYW8
			50%	80%	6e-64	*At*_LHCA5	Q9C639
			67%	98%	1e-118	*Cr*_LHCA7	Q84Y02
		g7087.t1	45%	84%	2e-50	*At*_LHCA5	Q9C639
			73%	92%	1e-104	*Cr*_LHCA9	A8ITV3
		g4083.t1	87%	50%	2e-63	*At*_LHCA5	Q9C639
			92%	46%	5e-62	*At*_LHCA4	P27521
			86%	52%	2e-61	*At*_LHCA2	Q9SYW8
			59%	99%	5e-94	*Cr*_LHCA8	Q75VY7
			53%	98%	1e-85	*Cr*_LHCA7	Q84Y02
LHC proteins putatively associated with PSII							
	LHCB1	g13401.t1	67%	100%	3e-122	*At*_LHCB1.1	P0CJ48
			67%	100%	3e-122	*At*_LHCB1.2	Q8VZ87
			69%	94%	3e-120	*At*_LHCB1.3	P04778
			66%	100%	3e-118	*At*_LHCB1.4	Q39142
			73%	99%	7e-139 3e-	*Cr*_LHCBM5	Q9ZSJ4
			72%	94%	129	*Cr*_LHCBM1	A8JCU4
		g4296.t1	48%	86%	2e-62	*At*_LHCB2.1	Q9SHR7
			48%	86%	2e-62	*At*_LHCB2.2	Q9S7J7
			48%	86%	2e-62	*At*_LHCB2.3	Q9XF87
			47%	88%	2e-67	*Cr*_LHCBM3	Q93WL4
			52%	78%	2e-66 7e-66	*Cr*_LHCBM4	A8J264
			52%	78%	2e-65	*Cr*_LHCBM6	A8J287
			52%	78%	3e-64	*Cr*_LHCBM8	A8J270
			51%	78%		*Cr*_LHCBM9	Q8S3T9
	LHCB2	g3288.t1	66%	89%	7e-126	*At*_LHCB2.1	Q9SHR7
			72%	77%	4e-125	*At*_LHCB2.2	Q9S7J7
			66%	89%	5e-125	*At*_LHCB2.3	Q9XF87
			83%	80%	1e-151	*Cr*_LHCBM1	A8JCU4
		g12130.t1	79%	86%	9e-128	*At*_LHCB2.1	Q9SHR7
			79%	86%	6e-128	*At*_LHCB2.2	Q9S7J7
			79%	85%	2e-127	*At*_LHCB2.3	Q9XF87
			79%	99%	9e-151	*Cr*_LHCBM3	Q93WL4
			81%	99%	8e-148	*Cr*_LHCBM4	A8J264
			83%	99%	1e-148	*Cr*_LHCBM6	A8J287
			80%	99%	1e-146	*Cr*_LHCBM8	A8J270
			79%	99%	9e-144	*Cr*_LHCBM9	Q8S3T9
		g7481.t1	76%	67%	2e-96	*At*_LHCB2.1	Q9SHR7
			76%	67%	2e-96	*At*_LHCB2.2	Q9S7J7
			75%	67%	1e-95	*At*_LHCB2.3	Q9XF87
			85%	67%	9e-109	*Cr*_LHCBM2	Q93WE0
			85%	67%	3e-108	*Cr*_LHCBM7	Q9AXF6

© 2026 The Author(s).
New Phytologist © 2026 New Phytologist Foundation.

Table 1 (Continued)

Description	Gene name	Gene ID Bs	Identity	Query cover	*E*-value	Compared to	UniProt KB
		g817.t1	76%	100%	3e-87	*At*_LHCB2.1	Q9SHR7
			76%	100%	4e-87	*At*_LHCB2.2	Q9S7J7
			75%	100%	2e-86	*At*_LHCB2.3	Q9XF87
			85%	98%	9e-97	*Cr*_LHCBM2	Q93WE0
			85%	98%	4e-96	*Cr*_LHCBM7	Q9AXF6
	LHCB3					*At*_LHCB3	Q9S7M0
Minor PSII Antenna Complex CP29	LHCB4	g4006.t1	58%	52%	1e-78	*At*_LHCB4.1	Q07473
			58%	52%	7e-80	*At*_LHCB4.2	Q9XF88
			53%	54%	2e-78	*At*_LHCB4.3	Q9S7W1
			73%	68%	3e-144	*Cr*_LHCB4	A8J6D1
Minor PSII Antenna Complex CP26	LHCB5	g6191.t1	56%	84%	1e-78	*At*_LHCB5	Q9XF89
			84%	100%	1e-177	*Cr*_LHCB5	Q9FEK6
Minor PSII Antenna Complex CP24	LHCB6	-				*At*_LHCB6	Q9LMQ2
	LHCB7	g118.t1	51%	73%	2e-95	*At*_LHCB7	Q9C9K1
			64%	96%	1e-165	*Cr*_LHCB7	A8I3C6
Photoprotective factors							
Stress-inducible light-harvesting complex proteins	PSBS	g2721.t1	46%	83%	1e-35	*At*_PSBS	Q9XF91
			60%	100%	6e-89	*Cr*_PSBS1	A8HPM2
			60%	100%	1e-88	*Cr*_PSBS2	A8HPM5
	LHCSR	g2890.t1	69%	90%	5e-117	*Cr*_LHCSR1	P93664
			68%	93%	2e-115	*Cr*_LHCSR3	A8J431
	ELIP2	g9419.t1	49%	59%	5e-24	*At*_ELIP2	Q94K66
	LIL3:1	g6210.t1	60%			At	Q9SYX1 Q6NKS4
	LIL3:2		57%				

almost unchanged PSII-LHCII fluorescence of *B. sudetica* in response to conditions known to induce State 2 indicates a minor role of antenna decoupling for PSII photoprotection (Allorent *et al.*, 2013; Ünlü *et al.*, 2014) in this organism.

The main NPQ components in *B. sudetica* were therefore determined to be qE and qI. Photoinhibitory quenching (qI) can be either attributed to the irreversible inactivation of PSII reaction centres or to the light-induced formation of zeaxanthin, which is responsible for the occurrence of a NPQ component qZ that relaxes slowly (Nilkens *et al.*, 2010) owing to the slow back-conversion into violaxanthin (Kromdijk *et al.*, 2016). The large fraction of the photoinhibitory NPQ component qI observed during high-light acclimation of *B. sudetica* (Fig. 3a) might thus actually represent the qZ component. To test this hypothesis, we analysed the effect of added DTT on the NPQ_{max} obtained for samples taken during the cultivation of *B. sudetica* in moderate–high light (Fig. 3c). At least for higher plant violaxanthin de-epoxidases (VDE), an inhibition by DTT has been reported (Yamamoto & Kamite, 1972), and a strong NPQ reduction by DTT could be observed for microalgal species belonging to the clades of chlorophyceae and trebouxiophyceae (Quaas *et al.*, 2015). Addition of DTT led to an up to 40% reduction of NPQ, observed for several samples taken during the high-light cultivation experiment (Fig. 3c; ±DTT; Bs). This indicated that VDE-dependent zeaxanthin accumulation contributes significantly to NPQ induction in *B. sudetica*. Following previous reports (Yamamoto & Kamite, 1972; Quaas *et al.*, 2015) and explained by the occurrence of an atypical VDE in *C. reinhardtii* (Li *et al.*, 2016), DTT addition to samples of *C. reinhardtii* resulted only in a mild reduction of NPQ (Fig. 3c; Cr). A more detailed analysis of the xanthophyll composition (Fig. 3d,e) of LL- and MHL-grown *B. sudetica* cells demonstrated that high-light exposure was accompanied by an increase of the violaxanthin pool size (Fig. 3d; left *y*-axis; dark grey bars) and an accumulation of zeaxanthin (white bars). The zeaxanthin content of HL-grown *C. reinhardtii* cells was much lower than that of *B. sudetica* (8.01 ± 2.67 mmol mol^{-1} Chl *a* in *C. reinhardtii* vs 32.54 ± 0.62 mmol mol^{-1} Chl *a* in *B. sudetica* at t_{29h}). In *B. sudetica*, the de-epoxidation state (DES) of violaxanthin strongly increased during high-light treatment (Fig. 3e; Bs), while the effects of high-light acclimation on DES were much smaller in *C. reinhardtii* (Fig. 3e; Cr). *B. sudetica* therefore displays an NPQ phenotype which strongly resembles the one found in vascular plants in terms of its rapid activation of qE (Fig. 2b), the minor contribution of qT (Fig. 3a,b), its dependence on light-induced zeaxanthin accumulation (Fig. 3c–e), and the occurrence of a qI/qZ component (Fig. 3a).

The nuclear genome of *B. sudetica* has been sequenced and annotated. We analysed the genetic repertoire with a focus on the light-harvesting antenna and the photoprotective machinery (Table 1). Among the photoprotective factors encoded by the nuclear genome of *B. sudetica* are homologues of the *A. thaliana* PSBS and *C. reinhardtii* LHCSR3 genes (Table 1; Figs S4, S5, alignments).

An analysis of PSBS function in *C. reinhardtii* demonstrated that this protein is part of a light-inducible qE system (Correa-Galvis *et al.*, 2016; Tibiletti *et al.*, 2016), whose activation is also dependent on the inorganic carbon supply in *Chlamydomonas* (Correa-Galvis *et al.*, 2016). Consistent with the rapid activation of NPQ in *B. sudetica* (Fig. 2b), mRNA levels remain almost

© 2026 The Author(s).
New Phytologist © 2026 New Phytologist Foundation.

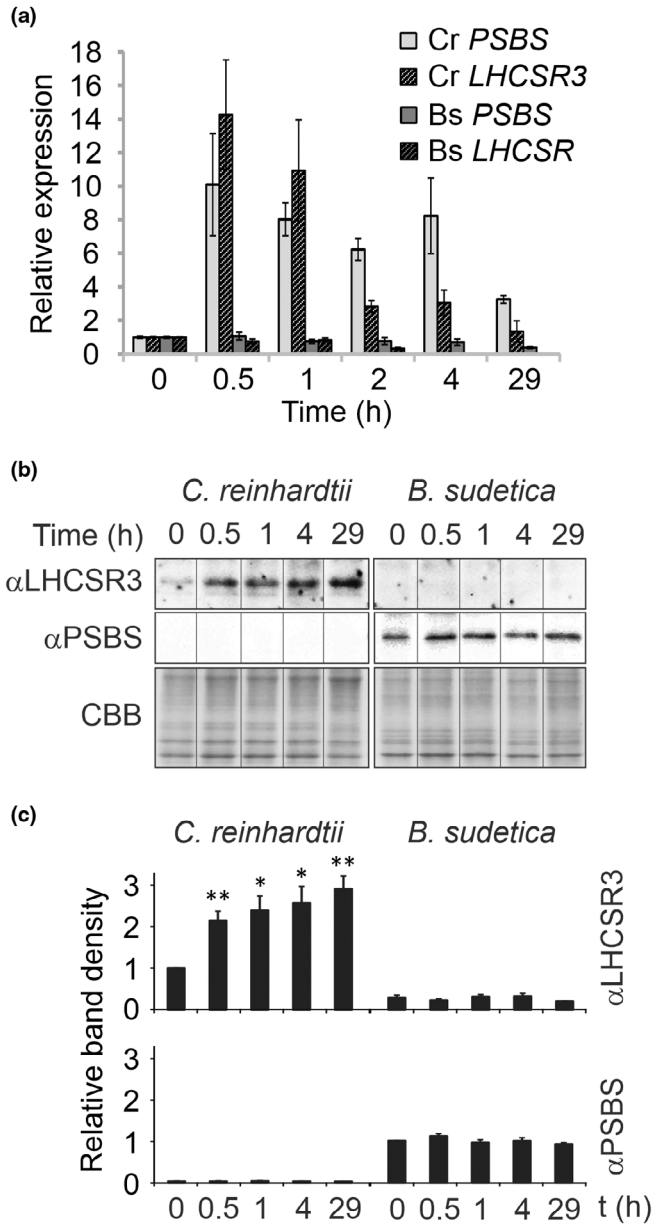


Fig. 4 *Botryosphaerella sudetica* expresses PSBS already under unstressed conditions. (a) Accumulation of *PSBS* and *LHCSR3* transcripts in *Chlamydomonas reinhardtii* and *B. sudetica* during the acclimation to excess light as determined by reverse transcription quantitative quantitative polymerase chain reaction (RT-qPCR). Cultures grown at 100 μmol photons m^{-2} s^{-1} (t_0) were transferred to a moderate high light intensity of 400 μmol photons m^{-2} s^{-1} ($t_{0.5}$–t_{29}) for the indicated times before RNA extraction. Data were normalised to the mRNA levels present at t_0 (set to 1). Shown are means ± SE (n = 2) from two biological and two technical replicates. (b) Accumulation of PSBS and LHCSR3 proteins analysed by immunoblotting. Protein loading was assessed by Coomassie Brilliant Blue (CBB) staining. (c) Densitometric analysis of immunoblot signals, normalised to the loading control. Mean values are derived from three independent experiments. Error bars represent SE (n = 3). Asterisks represent P-values from Student's t-test (*, $P < 0.05$; **, $P < 0.01$) relative to Cr t = 0 h for αLHCSR3 and Bs t = 0 h for αPSBS antibodies, which were set to 1. LHCSR, light-harvesting complex stress-related.

unaltered in response to excess light exposure, indicating a constitutive expression of this gene (Fig. 4a; *Bs*; *PSBS*). By contrast, the *C. reinhardtii PSBS* transcript level rapidly increased *c.* 10-fold upon light stress application (10.1 ± 3.04 at $t_{0.5h}$ vs 1 at t_0; Cr *PSBS*) and remained at a high level. Strong differences could also be noted for the genes *C.r.-LHCSR3* and its homologous gene in *B. sudetica* (Fig. 4a; Cr LHCSR3 vs Bs LHCSR). While LHCSR3 mRNA accumulated strongly (14.26 ± 3.26 vs 1 at t_0) within the first 30 min of high-light exposure ($t_{0.5}$ vs t_0; Cr), an induction could not be observed for *B. sudetica*. Both qE factors, PSBS and LHCSR, are therefore expressed constitutively in *B. sudetica* at the mRNA level.

The *B. sudetica* PSBS protein was already detectable under nonstress conditions (Fig. 4b; *B.s.*; PSBS; t_0), and protein levels remained unaltered during the exposure to light stress ($t_{0.5h}$–t_{29h}). In *C. reinhardtii*, however, PSBS accumulation could not be detected at all, which might be explained by the cultivation regime, including high (5% (v/v)) carbon dioxide provision, known to suppress PSBS accumulation in *C. reinhardtii* (Correa-Galvis *et al.*, 2016; Ruiz-Sola *et al.*, 2023). Although a high concentration of carbon dioxide was used for cultivation (Ruiz-Sola *et al.*, 2023), LHCSR3 protein accumulated in *C. reinhardtii* cells in response to high light, whereas LHCSR protein could not be detected in *B. sudetica*. To confirm the specificity of the applied antisera, different control experiments were performed. The PSBS antiserum could detect the PSBS protein expressed in *Arabidopsis thaliana*, *Physcomitrella patens*, and *B. sudetica*, when cultivated with 2% instead of 5% (v/v) CO_2. Only in high-light-treated Chlamydomonas cells LHCSR3 protein could be detected (Fig. S6). The antiserum raised against a peptide sequence derived from *C. reinhardtii* LHCSR3 could detect the recombinant *B. sudetica* protein in *E. coli* extracts (Fig. S7). An analogous experiment conducted with *E. coli* cells expressing recombinant *B. sudetica* PSBS confirmed specific PSBS detection by the applied antiserum (Fig. S8). It appears that the repression of LHCSR3 accumulation by high carbon dioxide concentrations depends on the type of growth medium used, as in the present case, Chu medium was employed instead of standard media (Sueoka, 1960) for cultivating *C. reinhardtii*. However, it must be stressed that we cannot exclude that PSBS levels increase during long-term light acclimation when time points beyond 1 d of light stress exposure are analysed, as studies conducted with *A. thaliana* demonstrated PSBS accumulation (20% to 80% relative to t_0) in a time range of several days after the onset of light stress (Ballottari *et al.*, 2007; Zia *et al.*, 2011).

Discussion

In the present study, we deeply investigated the photoprotective strategies applied by the chlorophycean green microalga *Botryosphaerella sudetica*. The strain UTEX 2629 was originally identified as *Botryococcus sudeticus*, after isolating it from a culture of *Botryococcus braunii* CCAP 807/1 (Vazquez-Duhalt & Greppin, 1987; Vasquez-Duhalt, 1991). As *B. sudetica* differs

© 2026 The Author(s).
New Phytologist © 2026 New Phytologist Foundation.

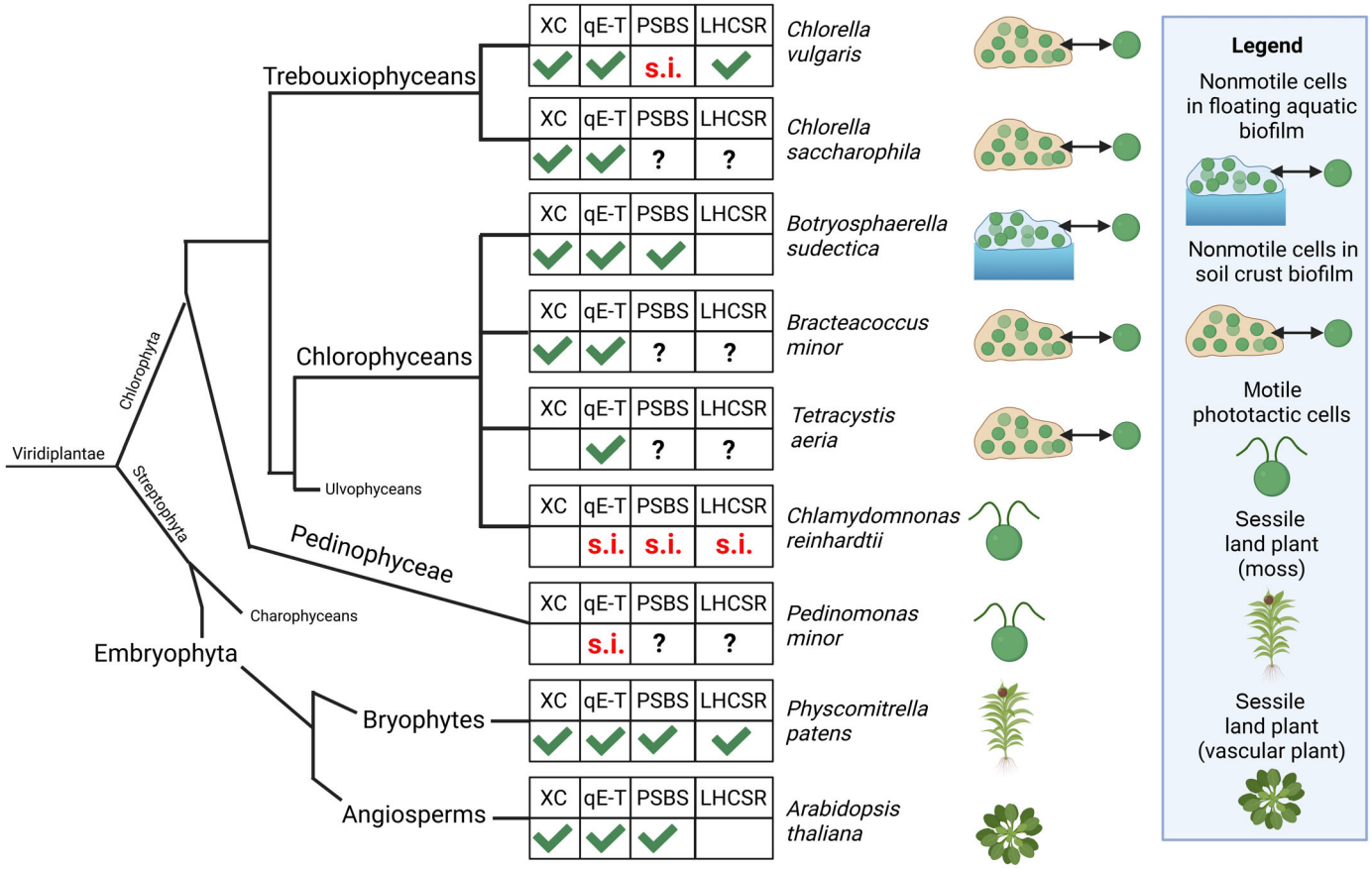


Fig. 5 Preferred type of energy-dependent quenching (qE) reflects the organism's lifestyle in the green plant lineage. Distinct examples of preferred qE strategies are indicated for organisms belonging to the *Viridiplantae* along with their phylogenetic relationships and lifestyle (see legend in figure). Dependence of qE on a xanthophyll cycle with zeaxanthin formation is indicated by a green check mark in the box 'XC'. Presence of a strong qE mechanism already under unstressed conditions is indicated by a green check mark, and qE requiring stress induction by 's.i.' in the box 'qE-T'. Accumulation of proteins PSBS or light-harvesting complex stress-related (LHCSR) under prestress conditions is indicated by a green check mark, while stress-induced accumulation is indicated by 's.i.'. References used for the synopsis are cited in the text. This figure was created in BioRender (BioRender.com/0n30f38).

markedly from *Botryococcus braunii* by forming clusters of round cells of varying size, while *B. braunii* has egg-shaped cells, the new genus *Botryosphaerella* was established by Silva (Silva, 1970).

Our data collectively show that *B. sudetica* differs strongly from *C. reinhardtii* regarding the NPQ mechanisms preferred to cope with high-light stress. Photoprotection in *B. sudetica* was shown to be more effective than in *C. reinhardtii*, as judged by the higher maximum quantum yields and oxygen evolution capacities (Fig. 1d) in high-light-acclimated *B. sudetica* vs *C. reinhardtii* cells. The predominant type of NPQ used by *B. sudetica* is energy-dependent quenching (qE), which is active without preacclimation and shows a high amplitude even in low-light-acclimated cells (Fig. 2b). A high quenching capacity of *B. sudetica* depends on zeaxanthin accumulation (Fig. 3c–e), which is another difference to *C. reinhardtii*. A zeaxanthin-dependence of NPQ has been observed in the Chlorophyceae *Bracteacoccus minor* before, by blocking violaxanthin de-epoxidation with DTT (Quaas *et al.*, 2015). Interestingly, this species also showed only a subtle difference in the NPQ capacity of low- and high-light-acclimated cells, pointing at a rather constitutive quenching mechanism (Quaas *et al.*, 2015).

This phenotype is also displayed by *B. sudetica*, and some features of its lifestyle might explain a preference for such a quenching mechanism. Photophobic responses, known for motile microalgae like *C. reinhardtii* or *Pedinomonas minor* (Leliaert *et al.*, 2012), might explain why some microalgae did not evolve constitutive qE mechanisms (Quaas *et al.*, 2015), because the opportunity of flagellated organisms to swim away from strong light sources (Kröger & Hegemann, 1994) is a very effective way of avoiding photodamage (Fig. 5).

Although flagellated cells from *B. sudetica* could be observed in dark conditions (Přibyl & Cepák, 2007), flagellated states could not be observed under the experimental conditions used in this study (Fig. 1a). The *B. sudetica* strain AVFF007 naturally forms biofilms as a quasi-sessile lifestyle (Muto *et al.*, 2017; Nojima *et al.*, 2017), but such a phenotype was not observed in the present study. The molecular basis for the rapidly inducible quenching found in *B. sudetica* is the expression of PSBS already under unstressed conditions (Fig. 4), whose function as a key factor for qE has already been described in vascular plants (Li *et al.*, 2000). The photoprotective role of the single LHCSR protein encoded by the nuclear genome of *B. sudetica* is currently difficult to

© 2026 The Author(s).
New Phytologist © 2026 New Phytologist Foundation.

address. Even under excess light conditions, the protein does not accumulate, thus not contributing to qE in high-light-acclimated *B. sudetica*. Unfortunately, gene knockdown and knock-out techniques are currently not available for *B. sudetica*, since such experiments could further prove the essentiality of PSBS for qE in *B. sudetica*.

While the constitutive high-amplitude quenching of vascular land plants like *Arabidopsis thaliana* (Fig. 5) relies on PSBS only (Li *et al.*, 2000, 2004), the evolutionary preceding moss *Physcomitrella patens* (Fig. 5) constitutively expresses PSBS and LHCSR proteins (Alboresi *et al.*, 2010; Pinnola *et al.*, 2013). There are several examples of constitutive quenching in nonmotile microalgae forming soil crust biofilms (Fig. 5), such as *Tetracystis aeria* (Quaas *et al.*, 2015; Wehr *et al.*, 2015), *Bracteacoccus minor* (Quaas *et al.*, 2015; Fuentes *et al.*, 2022), *Chlorella saccharophila* (Darienko *et al.*, 2010; Quaas *et al.*, 2015), or *Chlorella vulgaris* (Luo *et al.*, 2010; Hultberg *et al.*, 2014). RNA-seq analyses comparing the transcriptome of low-light- and high-light-acclimated *Chlorella vulgaris* cells revealed a constitutive expression of LHCSR and an inducible expression of PSBS, at least on the RNA level (Cecchin *et al.*, 2019).

Overall, it seems that the possession of constitutive qE mechanisms conferring an advantage in combination with a sessile lifestyle in habitats with frequent high-light exposure requires either constitutive PSBS or LHCSR expression (Fig. 5). In the moss *P. patens*, both quenching factors are constitutively expressed, and a single knock-out of LHCSR1 causes a great reduction in the amplitude of quenching (Alboresi *et al.*, 2010). In *C. reinhardtii*, the induction of LHCSR3 is sufficient for a functional qE mechanism (Peers *et al.*, 2009), but the transient expression of PSBS increases the fitness of cells under high-light conditions (Redekop *et al.*, 2022). Since only RNAseq data are available, it is currently unclear whether *Chlorella vulgaris* indeed accumulates LHCSR proteins under unstressed conditions. To confirm the hypothesis that motility is the evolutionary driver deciding about the preferred mode of NPQ, further microalgal species with contrasting lifestyles in regard to sessility need to be analysed.

The isolation of *B. sudetica* strains from cultures of the colonial green alga *Botryococcus braunii* suggests that both species inhabit similar environments (Vazquez-Duhalt & Greppin, 1987; Vasquez-Duhalt, 1991), where they are challenged by the same type of abiotic stress. Recently, a study on photoacclimation in *B. braunii* demonstrated that this species shows a substantial NPQ already under low-light conditions, which increases, however, significantly in response to excess light (van den Berg *et al.*, 2019). Like *B. sudetica*, *B. braunii* also encodes a PSBS (Phytozome 14: *Botryococcus braunii* v2.1; Bobra.139_1s0009, Bobra.0165s0088, Bobra.0082 s0023) but no LHCSR homologue (Browne *et al.*, 2017), while the expression profile of both proteins in response to stress remains to be analysed (van den Berg *et al.*, 2019).

In *C. reinhardtii*, a rapid detachment of large parts of the major light-harvesting antenna from PSII (Ünlü *et al.*, 2014) is seen as an efficient means of protecting PSII from photodamage following a sudden increase in light intensity, while the qE mechanism is being induced (Allorent *et al.*, 2013). In line with this view, a large contribution of qT to the overall NPQ in *C. reinhardtii* could be observed (Fig. 3b), while in *B. sudetica*, being equipped with a constitutive qE, qT involvement is rather small (Fig. 3b). Similarly, in the diatom *Phaeodactylum tricornutum*, which expresses a LHCSR protein constitutively (Bailleul *et al.*, 2010), state transitions contribute little to NPQ (Ting & Owens, 1993).

Acknowledgements

We thank R. Bassi (University of Verona) for the provision of antisera. We are grateful to the Center for Biotechnology (CeBiTec) at Bielefeld University for access to the Technology Platforms. *A. thaliana* protein samples were a kind gift of Prof. Dr. Karl-Josef Dietz (Bielefeld University) and *P. patens* protein samples were kindly provided by Prof. Dr. Michael Hippler (University of Münster). Open Access funding enabled and organized by Projekt DEAL.

Competing interests

None declared.

Author contributions

OB-K, HB and VK conceived and designed the research. OB-K isolated the *Botryosphaerella* microalga and conducted all *in silico* analyses. OB-K, HB and VK performed physiological studies, growth, and Chl fluorescence measurements. OB-K and HB conducted western blots and RT-qPCR experiments. SC and OB-K performed the pigment analyses. TB performed control experiments regarding the specificity of applied antisera. LW, OB-K and OK wrote the manuscript, with input from the co-authors.

ORCID

Thomas Baier https://orcid.org/0000-0002-5226-3035
Hanna Berger https://orcid.org/0000-0002-6933-7563
Olga Blifernez-Klassen https://orcid.org/0000-0003-1887-2491
Viktor Klassen https://orcid.org/0000-0003-2708-1835
Olaf Kruse https://orcid.org/0000-0001-9874-382X
Lutz Wobbe https://orcid.org/0000-0001-5141-9897

Data availability

The genome sequence has been submitted to NCBI as BioProject PRJNA1293936.

References

Alboresi A, Gerotto C, Giacometti GM, Bassi R, Morosinotto T. 2010. Physcomitrella patens mutants affected on heat dissipation clarify the evolution of photoprotection mechanisms upon land colonization. *Proceedings of the National Academy of Sciences, USA* **107**: 11128–11133.

Allorent G, Lefebvre-Legendre L, Chappuis R, Kuntz M, Truong TB, Niyogi KK, Ulm R, Goldschmidt-Clermont M. 2016. UV-B photoreceptor-mediated

© 2026 The Author(s).
New Phytologist © 2026 New Phytologist Foundation.

protection of the photosynthetic machinery in *Chlamydomonas reinhardtii*. *Proceedings of the National Academy of Sciences, USA* **113**: 14864–14869.

Allorent G, Tokutsu R, Roach T, Peers G, Cardol P, Girard-Bascou J, Seigneurin-Berny D, Petroutsos D, Kuntz M, Breyton C *et al.* 2013. A dual strategy to cope with high light in *Chlamydomonas reinhardtii*. *Plant Cell* **25**: 545–557.

Bailleul B, Rogato A, de Martino A, Coesel S, Cardol P, Bowler C, Falciatore A, Finazzi G. 2010. An atypical member of the light-harvesting complex stress-related protein family modulates diatom responses to light. *Proceedings of the National Academy of Sciences, USA* **107**: 18214–18219.

Ballottari M, Dall'Osto L, Morosinotto T, Bassi R. 2007. Contrasting behavior of higher plant photosystem I and II antenna systems during acclimation*. *The Journal of Biological Chemistry* **282**: 8947–8958.

van den Berg TE, Chukhutsina VU, van Amerongen H, Croce R, van Oort B. 2019. Light acclimation of the colonial green alga *Botryococcus braunii* strain Showa. *Plant Physiology* **179**: 1132–1143.

Berger H, Blifernez-Klassen O, Ballottari M, Bassi R, Wobbe L, Kruse O. 2014. Integration of carbon assimilation modes with photosynthetic light capture in the green alga *Chlamydomonas reinhardtii*. *Molecular Plant* **7**: 1545–1559.

Berger H, de Mia M, Morisse S, Marchand CH, Lemaire SD, Wobbe L, Kruse O. 2016. A light switch based on protein S-nitrosylation fine-tunes photosynthetic light harvesting in Chlamydomonas. *Plant Physiology* **171**: 821–832.

Blifernez-Klassen O, Chaudhari S, Klassen V, Wördenweber R, Steffens T, Cholewa D, Niehaus K, Kalinowski J, Kruse O. 2018. Metabolic survey of *Botryococcus braunii*: impact of the physiological state on product formation. *PLoS ONE* **13**: e0198976.

Blifernez-Klassen O, Klassen V, Wibberg D, Cebeci E, Henke C, Rückert C, Chaudhari S, Rupp O, Blom J, Winkler A *et al.* 2021. Phytoplankton consortia as a blueprint for mutually beneficial eukaryote-bacteria ecosystems based on the biocoenosis of *Botryococcus consortia*. *Scientific Reports* **11**: 1726.

Bonente G, Ballottari M, Truong TB, Morosinotto T, Ahn TK, Fleming GR, Niyogi KK, Bassi R. 2011. Analysis of LhcSR3, a protein essential for feedback de-excitation in the green alga *Chlamydomonas reinhardtii*. *PLoS Biology* **9**: e1000577.

Bonente G, Passarini F, Cazzaniga S, Mancone C, Buia MC, Tripodi M, Bassi R, Caffarri S. 2008. The occurrence of the psbS gene product in *Chlamydomonas reinhardtii* and in other photosynthetic organisms and its correlation with energy quenching. *Photochemistry and Photobiology* **84**: 1359–1370.

Browne DR, Jenkins J, Schmutz J, Shu S, Barry K, Grimwood J, Chiniquy J, Sharma A, Niehaus TD, Weiss TL *et al.* 2017. Draft nuclear genome sequence of the liquid hydrocarbon-accumulating green microalga *Botryococcus braunii* race B (Showa). *Genome Announcements* **5**: e00215-17.

Cecchin M, Marcolungo L, Rossato M, Girolomoni L, Cosentino E, Cuine S, Li-Beisson Y, Delledonne M, Ballottari M. 2019. Chlorella vulgaris genome assembly and annotation reveals the molecular basis for metabolic acclimation to high light conditions. *The Plant Journal* **100**: 1289–1305.

Correa-Galvis V, Redekop P, Guan K, Griess A, Truong TB, Wakao S, Niyogi KK, Jahns P. 2016. Photosystem II subunit PsbS is involved in the induction of LHCSR protein-dependent energy dissipation in *Chlamydomonas reinhardtii*. *Journal of Biological Chemistry* **291**: 17478–17487.

Darienko T, Gustavs L, Mudimu O, Menendez CR, Schumann R, Karsten U, Friedl T, Pröschold T. 2010. Chloroidium, a common terrestrial coccoid green alga previously assigned to Chlorella (Trebouxiophyceae, Chlorophyta). *European Journal of Phycology* **45**: 79–95.

Edelman M, Mattoo AK. 2008. D1-protein dynamics in photosystem II: the lingering enigma. *Photosynthesis Research* **98**: 609–620.

Elrad D, Niyogi KK, Grossman AR. 2002. A major light-harvesting polypeptide of photosystem II functions in thermal dissipation. *Plant Cell* **14**: 1801–1816.

Fuentes E, Pérez-Velón D, Prieto B. 2022. Effects of changes in UV-B radiation levels on biofilm-forming organisms commonly found in cultural heritage surfaces. *Environmental Research* **214**: 114061.

Goldschmidt-Clermont M, Bassi R. 2015. Sharing light between two photosystems: mechanism of state transitions. *Current Opinion in Plant Biology* **25**: 71–78.

Hultberg M, Asp H, Marttila S, Bergstrand K-J, Gustafsson S. 2014. Biofilm formation by *Chlorella vulgaris* is affected by light quality. *Current Microbiology* **69**: 699–702.

Klassen V, Blifernez-Klassen O, Wibberg D, Winkler A, Kalinowski J, Posten C, Kruse O. 2017. Highly efficient methane generation from untreated microalgae biomass. *Biotechnology for Biofuels* **10**: 186.

Kröger P, Hegemann P. 1994. Photophobic responses and phototaxis in Chlamydomonas are triggered by a single rhodopsin photoreceptor. *FEBS Letters* **341**: 5–9.

Kromdijk J, Głowacka K, Leonelli L, Gabilly ST, Iwai M, Niyogi KK, Long SP. 2016. Improving photosynthesis and crop productivity by accelerating recovery from photoprotection. *Science* **354**: 857–861.

Kruse O, Nixon PJ, Schmid GH, Mullineaux CW. 1999. Isolation of state transition mutants of *Chlamydomonas reinhardtii* by fluorescence video imaging. *Photosynthesis Research* **61**: 43–51.

Leliaert F, Smith DR, Moreau H, Herron MD, Verbruggen H, Delwiche CF, de Clerck O. 2012. Phylogeny and molecular evolution of the green algae. *Critical Reviews in Plant Sciences* **31**: 1–46.

Li XP, Björkman O, Shih C, Grossman AR, Rosenquist M, Jansson S, Niyogi KK. 2000. A pigment-binding protein essential for regulation of photosynthetic light harvesting. *Nature* **403**: 391–395.

Li X-P, Gilmore AM, Caffarri S, Bassi R, Golan T, Kramer D, Niyogi KK. 2004. Regulation of photosynthetic light harvesting involves intrathylakoid lumen pH sensing by the PsbS protein. *The Journal of Biological Chemistry* **279**: 22866–22874.

Li Z, Peers G, Dent RM, Bai Y, Yang SY, Apel W, Leonelli L, Niyogi KK. 2016. Evolution of an atypical de-epoxidase for photoprotection in the green lineage. *Nature Plants* **2**: 16140.

Liguori N, Roy LM, Opacic M, Durand G, Croce R. 2013. Regulation of light harvesting in the green alga *Chlamydomonas reinhardtii*: the C-terminus of LHCSR is the knob of a dimmer switch. *Journal of the American Chemical Society* **135**: 18339–18342.

Liu X, Nawrocki WJ, Croce R. 2024. The role of the pigment-protein complex LHCBM1 in nonphotochemical quenching in *Chlamydomonas reinhardtii*. *Plant Physiology* **194**: 936–944.

Luo W, Pröschold T, Bock C, Krienitz L. 2010. Generic concept in Chlorella-related coccoid green algae (Chlorophyta, Trebouxiophyceae). *Plant Biology* **12**: 545–553.

Malnoë A, Schultink A, Shahrasbi S, Rumeau D, Havaux M, Niyogi KK. 2018. The plastid lipocalin LCNP is required for sustained photoprotective energy dissipation in Arabidopsis. *Plant Cell* **30**: 196–208.

Maxwell K, Johnson GN. 2000. Chlorophyll fluorescence—a practical guide. *Journal of Experimental Botany* **51**: 659–668.

Müller P, Li XP, Niyogi KK. 2001. Non-photochemical quenching. A response to excess light energy. *Plant Physiology* **125**: 1558–1566.

Murchie EH, Lawson T. 2013. Chlorophyll fluorescence analysis: a guide to good practice and understanding some new applications. *Journal of Experimental Botany* **64**: 3983–3998.

Mussgnug JH, Thomas-Hall S, Rupprecht J, Foo A, Klassen V, McDowall A, Schenk PM, Kruse O, Hankamer B. 2007. Engineering photosynthetic light capture: impacts on improved solar energy to biomass conversion. *Plant Biotechnology Journal* **5**: 802–814.

Muto M, Nojima D, Yue L, Kanehara H, Naruse H, Ujiro A, Yoshino T, Matsunaga T, Tanaka T. 2017. Potential of water surface-floating microalgae for biodiesel production: Floating-biomass and lipid productivities. *Journal of Bioscience and Bioengineering* **123**: 314–318.

Nilkens M, Kress E, Lambrev P, Miloslavina Y, Müller M, Holzwarth AR, Jahns P. 2010. Identification of a slowly inducible zeaxanthin-dependent component of non-photochemical quenching of chlorophyll fluorescence generated under steady-state conditions in Arabidopsis. *Biochimica et Biophysica Acta* **1797**: 466–475.

Niyogi KK, Bjorkman O, Grossman AR. 1997a. Chlamydomonas Xanthophyll Cycle Mutants Identified by Video Imaging of Chlorophyll Fluorescence Quenching. *Plant Cell* **9**: 1369–1380.

Niyogi KK, Björkman O, Grossman AR. 1997b. The roles of specific xanthophylls in photoprotection. *Proceedings of the National Academy of Sciences, USA* **94**: 14162–14167.

Nojima D, Ishizuka Y, Muto M, Ujiro A, Kodama F, Yoshino T, Maeda Y, Matsunaga T, Tanaka T. 2017. Enhancement of biomass and lipid

© 2026 The Author(s).
New Phytologist © 2026 New Phytologist Foundation.

productivities of water surface-floating microalgae by chemical mutagenesis. *Marine Drugs* **15**: 151.

Peers G, Truong TB, Ostendorf E, Busch A, Elrad D, Grossman AR, Hippler M, Niyogi KK. 2009. An ancient light-harvesting protein is critical for the regulation of algal photosynthesis. *Nature* **462**: 518–521.

Petroutsos D, Tokutsu R, Maruyama S, Flori S, Greiner A, Magneschi L, Cusant L, Kottke T, Mittag M, Hegemann P *et al.* 2016. A blue-light photoreceptor mediates the feedback regulation of photosynthesis. *Nature* **537**: 563–566.

Pinnola A, Dall'Osto L, Gerotto C, Morosinotto T, Bassi R, Alboresi A. 2013. Zeaxanthin binds to light-harvesting complex stress-related protein to enhance nonphotochemical quenching in Physcomitrella patens. *Plant Cell* **25**: 3519–3534.

Přibyl P, Cepák V. 2007. Evidence for sexual reproduction and zoospore formation in *Botryosphaerella sudetica* UTEX 2629, previously assigned to the genus Botryococcus (Chlorophyceae, Chlorophyta). *Nova Hedwigia* **85**: 63–71.

Quaas T, Berteotti S, Ballottari M, Flieger K, Bassi R, Wilhelm C, Goss R. 2015. Non-photochemical quenching and xanthophyll cycle activities in six green algal species suggest mechanistic differences in the process of excess energy dissipation. *Journal of Plant Physiology* **172**: 92–103.

Redekop P, Rothhausen N, Rothhausen N, Melzer M, Mosebach L, Dülger E, Bovdilova A, Caffarri S, Hippler M, Jahns P. 2020. PsbS contributes to photoprotection in *Chlamydomonas reinhardtii* independently of energy dissipation. *Biochimica et Biophysica Acta, Bioenergetics* **1861**: 148183.

Redekop P, Sanz-Luque E, Yuan Y, Villain G, Petroutsos D, Grossman AR. 2022. Transcriptional regulation of photoprotection in dark-to-light transition-More than just a matter of excess light energy. *Science Advances* **8**: eabn1832.

Rochaix J-D. 2011. Regulation of photosynthetic electron transport. *Biochimica et Biophysica Acta* **1807**: 375–383.

Ruiz-Sola MÁ, Flori S, Yuan Y, Villain G, Sanz-Luque E, Redekop P, Tokutsu R, Küken A, Tsichla A, Kepesidis G *et al.* 2023. Light-independent regulation of algal photoprotection by CO_2 availability. *Nature Communications* **14**: 1977.

Silva PC. 1970. Remarks on algal Nomenclature. IV. *Taxon* **19**: 941–945.

Silva PC. 1980. Remarks on algal nomenclature VI. *Taxon* **29**: 121–145.

Sueoka N. 1960. Mitotic replication of deoxyribonucleic acid in *Chlamydomonas reinhardi. Proceedings of the National Academy of Sciences, USA* **46**: 83–91.

Tibiletti T, Auroy P, Peltier G, Caffarri S. 2016. *Chlamydomonas reinhardtii* PsbS protein is functional and accumulates rapidly and transiently under high light. *Plant Physiology* **171**: 2717–2730.

Ting CS, Owens TG. 1993. Photochemical and nonphotochemical fluorescence quenching processes in the diatom *Phaeodactylum tricornutum. Plant Physiology* **101**: 1323–1330.

Truong TB. 2011. Investigating the role(s) of LHCSRs in *Chlamydomonas reinhardtii.*

Ünlü C, Drop B, Croce R, van Amerongen H. 2014. State transitions in *Chlamydomonas reinhardtii* strongly modulate the functional size of photosystem II but not of photosystem I. *Proceedings of the National Academy of Sciences, USA* **111**: 3460–3465.

Vasquez-Duhalt R. 1991. Effet de la lumière sur l'accumulation de lipides neutres et la composition de la biomasse chez l'algue *Botryococcus sudeticus* (Chlorophyceae). *Cryptogamie Algologie* **12**: 109–119.

Vazquez-Duhalt R, Greppin H. 1987. Growth and production of cell constituents in batch cultures of *Botryococcus sudeticus. Phytochemistry* **26**: 885–889.

Wehr JD, Sheath RG, Kociolek JP. 2015. *Freshwater algae of North America. Ecology and classification.* Amsterdam, the Netherlands: Academic Press.

Wilson S, Kim E, Ishii A, Ruban AV, Minagawa J. 2023. Overexpression of LHCSR and PsbS enhance light tolerance in *Chlamydomonas reinhardtii. Journal of Photochemistry and Photobiology. B, Biology* **244**: 112718.

Wobbe L, Bassi R, Kruse O. 2016. Multi-level light capture control in plants and green algae. *Trends in Plant Science* **21**: 55–68.

Wobbe L, Blifernez O, Schwarz C, Mussgnug JH, Nickelsen J, Kruse O. 2009. Cysteine modification of a specific repressor protein controls the translational status of nucleus-encoded LHCII mRNAs in Chlamydomonas. *Proceedings of the National Academy of Sciences, USA* **106**: 13290–13295.

Wollman F-A, Bennoun P. 1982. A new chlorophyll-protein complex related to Photosystem I in *Chlamydomonas reinhardii. Biochimica et Biophysica Acta – Bioenergetics* **680**: 352–360.

Wollman FA, Delepelaire P. 1984. Correlation between changes in light energy distribution and changes in thylakoid membrane polypeptide phosphorylation in *Chlamydomonas reinhardtii. The Journal of Cell Biology* **98**: 1–7.

Yamamoto HY, Kamite L. 1972. The effects of dithiothreitol on violaxanthin de-epoxidation and absorbance changes in the 500-nm region. *Biochimica et Biophysica Acta* **267**: 538–543.

Zia A, Johnson MP, Ruban AV. 2011. Acclimation- and mutation-induced enhancement of PsbS levels affects the kinetics of non-photochemical quenching in *Arabidopsis thaliana. Planta* **233**: 1253–1264.

Supporting Information

Additional Supporting Information may be found online in the Supporting Information section at the end of the article.

Fig. S1 Light microscopic image of *Botryosphaerella sudetica* and *Chlamydomonas reinhardtii* cells.

Fig. S2 Fluorescence traces with dark recovery.

Fig. S3 Substantial differences between *B. sudetica* and *C. reinhardtii* regarding the state transitions process.

Fig. S4 Sequence alignments of *B. sudetica* PSBS protein with homologues from a. *A. thaliana* and *C. reinhardtii.*

Fig. S5 Sequence alignments of *B. sudetica* LHCSR protein with LHCSR1 and LHCSR3 from *C. reinhardtii.*

Fig. S6 Accumulation of PSBS and LHCSR3 proteins analysed by immunoblotting.

Fig. S7 Immunoblot analysis of recombinant Bs-LHCSR (His_6-tagged) protein.

Fig. S8 Immunoblot analysis of recombinant Bs-PSBS (His_6-tagged) protein.

Table S1 DNA oligonucleotide sequences.

Please note: Wiley is not responsible for the content or functionality of any Supporting Information supplied by the authors. Any queries (other than missing material) should be directed to the *New Phytologist* Central Office.

Disclaimer: The New Phytologist Foundation remains neutral with regard to jurisdictional claims in maps and in any institutional affiliations.

See also the Commentary on this article by Jin, **251**: 5–7.

© 2026 The Author(s).
New Phytologist © 2026 New Phytologist Foundation.